PHYSICAL REVIEW B **68**, 064514 (2003)

Magnetotransport properties of doped $RuSr_2GdCu_2O_8$

J. E. McCrone,[1] J. L. Tallon,[2] J. R. Cooper,[1] A. C. MacLaughlin,[3] J. P. Attfield,[3] and C. Bernhard[4]
[1]*IRC in Superconductivity, Cambridge University, Cambridge CB3 0HE, United Kingdom*
[2]*Industrial Research Ltd., P.O. Box 31310, Lower Hutt, New Zealand*
[3]*IRC in Superconductivity and Department of Chemistry, Cambridge University, Cambridge CB2 IEW, United Kingdom*
[4]*Max-Planck-Institut für Festkörperforschung, D-70569 Stuttgart, Germany*
(Received 27 February 2003; published 26 August 2003)

$RuSr_2GdCu_2O_8$, in which magnetic order and superconductivity coexist with $T_{mag} \gg T_c$, is a complex material which poses new and important questions to our understanding of the interplay between magnetic and superconducting order. Resistivity, Hall-effect, and thermopower measurements on sintered ceramic $RuSr_2GdCu_2O_8$ are presented, together with results on a broad range of substituted analogs. The Hall effect and thermopower both show anomalous decreases below T_{mag}, which may be explained within a simple two-band model by a transition from localized to more itinerant behavior in the RuO_2 layer at T_{mag}.

DOI: 10.1103/PhysRevB.68.064514 PACS number(s): 74.25.Fy, 74.25.Ha, 74.72.Jt

I. INTRODUCTION

Soon after the first successful synthesis[1] of $RuSr_2GdCu_2O_8$, the material was found to display not only superconductivity ($T_c \simeq 45$ K) but coexisting magnetic order with $T_{mag} \simeq 135$ K.[2,3] Evidence accumulated from static magnetization, muon spin rotation,[3] and from[4] Gd-electron-spin-resonance[4] studies showing that the magnetism is a spatially uniform bulk property. Specific-heat measurements[2] and the diamagnetic shielding fraction at low temperatures[3,5,6] indicate that the superconductivity is also a bulk property, and that the two phases therefore coexist on a truly microscopic scale. An initial neutron diffraction study eliminated the possibility of ferromagnetic (FM) order with the Ru moments lying in the RuO_2 plane, but did not rule out FM alignment with the moments parallel to the *c* axis, canted ferromagnetism, or itinerant ferromagnetism.[7] Subsequent polarized neutron diffraction data[8] have thrown the debate on $RuSr_2GdCu_2O_8$ wide open by appearing to show that the underlying ordering of the Ru moments below the magnetic transition is in fact *G*-type antiferromagnetic (antiparallel nearest-neighbor ordering in all three crystallographic directions). Finally, more recent neutron measurements on $RuSr_2YCu_2O_8$ confirmed that there is indeed a FM component of about $0.28\mu_B$ which is about (1/5)th of the antiferromagnetic (AFM) component of $1.2\mu_B$.[9] The magnetic order shows a rather strong and unusual response to an applied magnetic field, with the FM component growing rapidly in strength and dominating over the AFM already at 2 T. Whatever the nature of its magnetism, the discovery of this material is an exciting development which poses new and important questions to our understanding of the interplay between magnetic and superconducting (SC) order.

Magnetoresistance (MR), Hall-effect, and thermopower (TEP) measurements on undoped sintered ceramic $RuSr_2GdCu_2O_8$ were presented previously.[10] Above T_{mag} the MR is negative and proportional to the square of the Ru magnetization and was ascribed to spin scattering of the carriers. A model for dilute magnetic alloys was used to extract a value ($\geqslant 25$ meV) for the exchange interaction between the Ru moments and the carriers. Below T_{mag} the Hall effect and TEP both fall anomalously. It will be shown that these data may be explained within a simple two-band model by a transition from localized to more itinerant behavior in the RuO_2 layer at T_{mag}. Evidence for delocalized carriers within the RuO layers has also been obtained from other transport and microwave absorption studies[11] as well as from Ru-NMR (nuclear-magnetic-resonance) measurements where clear anomalies in the Ru-NMR relaxation rate occur near T_c.[12] This suggests that the Ru nuclear moments experience a sizable hyperfine coupling to the charge carriers that enter the SC state.

The magnetothermopower reveals an extremely unusual variation of T_c with applied field:[6] T_c actually *increases* by ~ 4 K as the applied field is increased to 2 T. The increase saturates along with the Ru magnetization, suggesting that the onset of Ru magnetic order reduces a magnetic pair-breaking effect in the CuO_2 layer.

The carrier concentration in $RuSr_2GdCu_2O_8$ and its magnetic and SC properties, structural deformations, and so forth may be altered by cation substitution. Examining the transport properties of such samples should lead to a better understanding of the parent material. In this paper we present magnetotransport measurements on substituted $RuSr_2GdCu_2O_8$. It will be shown that the data strongly support a simple two-band model in which the Hall effect and TEP of each sample are determined by the properties of the CuO_2 and RuO_2 layers, weighted appropriately by their conductivities. The model indicates that the RuO_2 layer in the undoped material is very poorly conducting at room temperature, with $\sigma_{Ru} \sim 0.1\sigma_{Cu}$, increasing to $\sim 0.3\sigma_{Cu}$ or higher at low temperature. While in most of the samples studied the CuO_2 layer remains the better conductor at all temperatures, we find that the RuO_2 layer dominates the conductivity below T_{mag} in a sample with 10% Ce^{4+} substituted for Gd^{3+}.

II. EXPERIMENTAL METHODS

Phase-pure sintered pellets of $RuSr_2GdCu_2O_8$ were synthesized as described previously via solid-state reaction of a stoichiometric mixture of high-purity metal oxides and

TABLE I. Substituted variants of $RuSr_2GdCu_2O_8$ studied in this work.

Composition	Substituted site
$Ru_{0.6}Sn_{0.4}Sr_2GdCu_2O_8$	40% Sn for Ru
$Ru_{0.8}Sn_{0.2}Sr_2GdCu_2O_8$	20% Sn for Ru
$Ru_{0.925}Sn_{0.075}Sr_2GdCu_2O_8$	7.5% Sn for Ru
$Ru_{0.975}Sn_{0.025}Sr_2GdCu_2O_8$	2.5% Sn for Ru
$Ru_{0.8}Nb_{0.2}Sr_2GdCu_2O_8$	20% Nb for Ru
$Ru_{0.9}Nb_{0.1}Sr_2GdCu_2O_8$	10% Nb for Ru
$RuSr_2Gd_{0.8}Ce_{0.2}Cu_2O_8$	20% Ce for Gd
$RuSr_2Gd_{0.9}Ce_{0.1}Cu_2O_8$	10% Ce for Gd
$RuSr_2EuCu_2O_8$	100% Eu for Gd
$RuSr_2Gd_{0.6}Dy_{0.4}Cu_2O_8$	40% Dy for Gd
$RuSr_2Gd_{0.9}Y_{0.1}Cu_2O_8$	10% Y for Gd
$RuSr_2GdCu_{1.9}Li_{0.1}O_8$	5% Li for Cu

$SrCO_3$.[3,13] The doped samples, listed in Table I, were produced similarly; the compositions given are nominal. A final extended anneal at 1060 °C in flowing high-purity O_2 produces a marked improvement in the crystallinity of the undoped material, resulting in a higher resistive T_c [as defined by $\rho(T)=0$] but no significant change in the thermodynamic T_c.[2]

Bars of approximate dimensions $4\times1\times0.7$ mm^3 were cut from the sintered pellets using a diamond wheel, then polished down to a thickness of ~150 μm in order to increase the measured Hall voltage. They were mounted on quartz substrates in a standard six-contact configuration allowing both resistance and Hall voltage to be measured simultaneously. The contacts were made using 25-μm gold wire and *Dupont 6838* conducting epoxy, cured in air at 450 °C for 6 min, giving contact resistances <1 Ω.

Resistivity and Hall-effect measurements were made using an ac current source, low-noise transformers, and lock-in amplifiers. A frequency of ~77 Hz was used to avoid mains pickup, with current densities of around 0.25 A cm^{-2}. The Hall coefficient R_H was usually measured by stabilizing the temperature and field (10 T unless stated otherwise), then measuring the Hall voltage with the sample rotated by 0 ° and 180° with respect to the field. The Hall coefficient is then given by $R_H=(V_0-V_{180})t/2IB$, where B is the magnetic field, t is the sample thickness, and I is the current. This method eliminates the MR of the sample, and the offset voltage from ρ_{xx} due to contact misalignment. Where R_H was measured as a function of field, this was swept to both positive and negative values and $R_H(B)$ determined from V_B-V_{-B}.

TEP measurements were made by the ''toggled'' heating method.[14,15] Two 25-μm chromel-alumel thermocouples, attached to the sample with small blobs of silver paint, measure both the thermal emf and temperature gradient, ensuring that these are measured between the same two points. The sample is first stabilized at the measurement temperature, a small thermal gradient is applied, and the resulting thermal emf measured. The thermal gradient is then reversed, allowing slowly changing thermal emf's in the cryostat wires to be nulled out. A ''rest state'' was added whereby both ends of the sample were heated at half power, providing two extra measurement points. Adding this state keeps the total power dissipation into the stage constant, avoiding fluctuation of its temperature when the heater currents are changed.

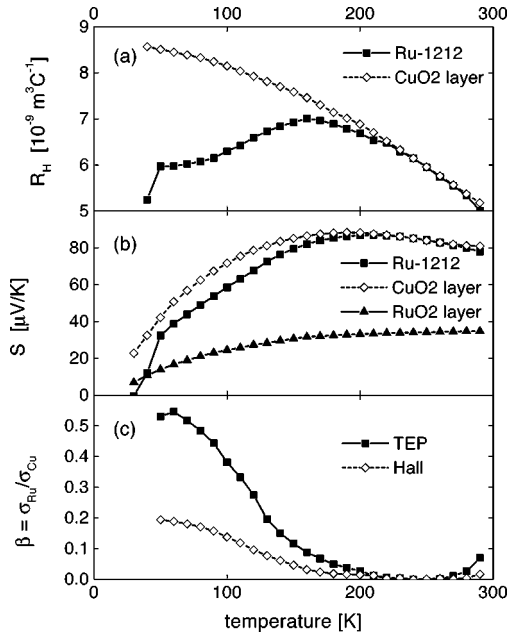

FIG. 1. (a) Hall-effect and (b) thermopower data for $RuSr_2GdCu_2O_8$, together with estimated values of the CuO_2 and RuO_2 layer properties as described in the text. Panel (c) shows the ratio $\beta=\sigma_{Ru}/\sigma_{Cu}$ calculated in the two-band model, assuming $\sigma_{Ru}\simeq0$ well above T_{mag}.

III. RESULTS

A. Transport measurements on pure $RuSr_2GdCu_2O_8$

Hall-effect, thermopower, and resistivity data for undoped $RuSr_2GdCu_2O_8$ are shown in Fig. 1. The room-temperature value of the TEP implies a hole concentration p_{Cu} of 0.06–0.07 holes/Cu,[16] while its temperature dependence is typical of other high-T_c materials, with the exception of the unusual linear temperature dependence below T_{mag}. The overall magnitude and temperature dependence of the Hall coefficient is consistent with a doping level, p_{Cu}, of $\simeq0.07$ holes/Cu, as inferred from the room-temperature TEP. R_H displays a high-T_c-like temperature dependence well above T_{mag}. However, below about 170 K there is an anomalous downturn in R_H which is not seen in typical high-T_c data. The so-called ''anomalous'' Hall effect observed in magnetic materials has been measured and discounted as the cause of this downturn.[17] Alternatively, it is due to charge delocalization in the RuO_2 plane occurring near the magnetic transition, or due to charge transfer into the CuO_2 layers. It will be shown that a two-band model, with a localized to itinerant transition occurring at T_{mag} in the RuO_2 layer, can explain both these and the TEP data.

1. The conductivity of the RuO_2 layer

The bands in this model are those formed by carriers in the Cu and Ru orbitals; the overall TEP and Hall effect are

given by the sum of the CuO_2 and RuO_2 layer values, weighted by the layer conductivities as follows:[18,19]

$$R_H = \frac{R_H^{\mathrm{Ru}}(\sigma_{xx}^{\mathrm{Ru}})^2 + R_H^{\mathrm{Cu}}(\sigma_{xx}^{\mathrm{Cu}})^2}{(\sigma_{xx}^{\mathrm{Ru}} + \sigma_{xx}^{\mathrm{Cu}})^2}, \tag{1}$$

$$S = \frac{S^{\mathrm{Ru}}\sigma_{xx}^{\mathrm{Ru}} + S^{\mathrm{Cu}}\sigma_{xx}^{\mathrm{Cu}}}{\sigma_{xx}^{\mathrm{Ru}} + \sigma_{xx}^{\mathrm{Cu}}}. \tag{2}$$

With some reasonable estimates of the RuO_2 and CuO_2 layer properties, it is possible to use this model and the measured room-temperature Hall effect and TEP to place a limit on the conductivity of the RuO_2 layer. To do this we assume that the Hall coefficient of the RuO_2 layer is approximately zero (the maximum value observed in other two-dimensional Ru oxides studied to date is 5×10^{-10} m^3 C^{-1}).[20–22] With this assumption in Eq. (1), the conductivity of the RuO_2 layer may be estimated from

$$\frac{\sigma_{xx}^{\mathrm{Ru}}}{\sigma_{xx}^{\mathrm{Cu}}} = \sqrt{\frac{R_H^{\mathrm{Cu}}}{R_H}} - 1,$$

$$R_H^{\mathrm{Ru}} \ll R_H^{\mathrm{Cu}}; \quad \sigma_{xx}^{\mathrm{Ru}} < \sigma_{xx}^{\mathrm{Cu}}. \tag{3}$$

The ratio of the Hall coefficient of the CuO_2 layers, R_H^{Cu}, to the measured value R_H caused by the presence of the RuO_2 layer is hard to estimate due to the uncertain doping state in $RuSr_2GdCu_2O_8$ and the spread of values of R_H^{Cu}, for a given doping level, in the literature.[23–25] Given these uncertainties, a reasonable range of values of R_H^{Cu}/R_H is 1–1.4, giving $\sigma_{xx}^{\mathrm{Ru}}$ in the range $(0–0.18)\sigma_{xx}^{\mathrm{Cu}}$. The summary of R_H^{Cu} values in the review by Cooper and Loram[26] would favor the low end of this range.

For this range of conductivity in the RuO_2 layer, Eq. (2) predicts that the measured net TEP lies some 0–8 $\mu V\,K^{-1}$ below the intrinsic CuO_2 layer value, i.e., $75 \leqslant S_{290}^{\mathrm{Cu}} \leqslant 83$. It is very unlikely that S_{290}^{Cu} lies in the upper half of this range: a value of $S = 83$ $\mu V\,K^{-1}$ would imply an extremely small hole concentration for which a T_c as high as 46 K would be extraordinary.

Having placed a limit on the conductivity one can use a two-dimensional model to determine $k_F l$, the product of the Fermi wave vector with the mean free path for the RuO_2 layers. This quantity gives an indication as to whether the carriers are localized or itinerant and for a cylindrical Fermi surface may be written as

$$k_F l = \sigma \frac{2\pi\hbar c}{e^2}, \tag{4}$$

where c is the separation of the planes. Data in the literature for the *ab*-plane resistivity of underdoped $YBa_2Cu_3O_{7-\delta}$ films and single crystals, with $p \simeq 0.07$, give a consistent value of 1.2 mΩ cm at room temperature[24,27–29] giving $k_F l_{\mathrm{Cu}} = 1.3$, near the limit of localization. In fact, in only slightly more underdoped samples one sees a semiconducting upturn at low temperatures. Given the range of ratios of $\sigma_{xx}^{\mathrm{Ru}}$ to $\sigma_{xx}^{\mathrm{Cu}}$ derived from the Hall effect, $k_F l_{\mathrm{Ru}} = 0–0.45$ at room temperature. The TEP data suggest that the true value is at the low end of this range, indicating that the carriers in the RuO_2 layers are at best very poorly metallic.

2. Temperature dependence of σ_{Ru}

Having established that the room-temperature conductivity of the RuO_2 layer is close to zero, typical $S(T)$ and $R_H(T)$ data for high-T_c superconductors may be scaled so that the room-temperature values match those of $RuSr_2GdCu_2O_8$. The differences below T_{mag} may then be used to follow σ_{Ru} as a function of temperature.

Typical Hall-effect data for the CuO_2 layer have been taken from measurements on sintered Ca-doped $YBa_2Cu_3O_{7-\delta}$, while R_H^{Ru} will be set to zero, its value in other RuO_2 layer compounds being much lower than R_H^{Cu}.[20–22] Typical S^{Cu} data are approximated by measurements on sintered $YBa_2Cu_3O_{7-\delta}$ with $\delta = 0.53$,[26] multiplied by 1.12 to match the high-temperature $RuSr_2GdCu_2O_8$ data. Finally, S^{Ru} is approximated by data measured on a sintered sample of $SrRuO_3$, which displays a magnitude and temperature dependence similar to that of Sr_2RuO_4.[30] All these data are shown in Fig. 1, together with the resulting $\beta(T) = \sigma_{\mathrm{Ru}}/\sigma_{\mathrm{Cu}}$ calculated from Eqs. (1) and (2).

Given the uncertainties in the approximated RuO_2 and CuO_2 layer properties the two $\beta(T)$ curves calculated independently from the drops in $S(T)$ and $R_H(T)$ agree well qualitatively. If TEP data for a sample of 20% Sn-doped $RuSr_2GdCu_2O_8$, in which we shall argue that σ_{Ru} is strongly suppressed below T_{mag}, are used to approximate S^{Cu}, the agreement is also quantitative. Because the TEP is a less sensitive function of β than the Hall-effect, the difference between S^{1212} and S^{Cu} is quite small compared with that between R_H^{1212} and R_H^{Cu}. Thus the value of β calculated from the TEP data is more sensitive to inaccuracy in the assumed S^{Cu} data. This explains why using the (only slightly different) 20% Sn-doped data to approximate $S^{\mathrm{Cu}}(T)$ results in a better match to $\beta(T)$ calculated from the Hall-effect. Whichever data are used, the results show a rapid rise in the relative conductivity of the RuO_2 layer below 150 K, to $\sim 0.3\sigma_{\mathrm{Cu}}$ or higher.

B. Transport measurements on substituted $RuSr_2GdCu_2O_8$

1. Sn-doped $RuSr_2GdCu_2O_8$

The diamagnetic Sn^{4+} ion substitutes for Ru in solid solution, and is slightly larger in size than $Ru^{4+/5+}$. The effects of doping the Ru site are of extreme interest given the current debate regarding the spin and charge configuration of the Ru ions.[31–33]

We note that the Sn-doped samples studied here were from two sources prepared with slightly different annealing strategies. Comparison of their sample resistivities is therefore not necessarily meaningful, as annealing strongly affects the grain-boundary conductivity of $RuSr_2GdCu_2O_8$.[10] In general, the resistivity of sintered high-T_c materials is also affected by sample density.[34,35]

For the 2.5% and 7.5% samples the resistivity (Fig. 2) is metallic, and similar in magnitude to the undoped sample.

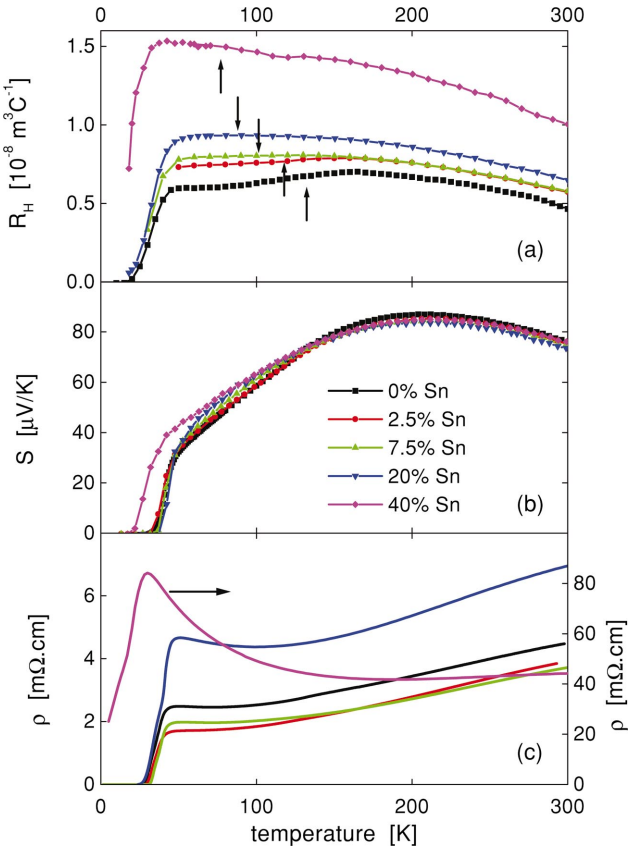

FIG. 2. (Color) (a) Hall-effect, (b) thermopower, and (c) resistivity data for Sn-doped samples of $RuSr_2GdCu_2O_8$.

The 20% sample has a higher resistivity and shows a small semiconducting upturn at low temperatures, while both the magnitude and upturn are far larger for the 40% sample. Estimating T_c from the onset of the resistive transition reveals a gradual increase from 40.5 K for the 2.5% sample to 43.5 K for the 20% sample, while the 40% sample has a reduced T_c of just 30 K.

The TEP $S(T)$ and Hall effect $R_H(T)$ are much less affected by grain boundaries than the resistivity. In conventional high-T_c materials they closely reflect bulk CuO_2 layer properties in conventional high-T_c materials.[35,36]

The Hall-effect data show a slow and monotonic decrease in T_c with increasing Sn concentration, but it should be remembered that these data were taken in a field of 10 T and only partly reflect the zero-field T_c. The vertical arrows in Fig. 2 (and in subsequent figures) show the location of the magnetic transition. The TEP data show that T_c (defined by the maximum in the derivative) rises by ~ 4 K in going from the 2.5% sample to the 20% sample, in good agreement with the resistivity data. The 40% sample shows a much lower transition temperature, both in R_H and S. The increase in T_c with Sn concentration is attributed to a transfer of holes into the CuO_2 layer,[37] though we observe a smaller increase than the ~ 12 K reported previously.[37,38] In the earlier studies T_c was defined from the resistivity onset, and the T_c values obtained for low doping levels were significantly lower, possibly due to granularity.

On examining the temperature and doping dependence of the normal-state properties, one immediately observes that the room-temperature TEP S_{290} is little changed by the addition of Sn. This result is strange given the rise of ~ 4 K in T_c as the doping level is increased to 20%. The change in the Hall effect is also counterintuitive: the 30% increase in going from 0 to 20% Sn would normally indicate a *decrease* in hole concentration. This apparent paradox is resolved when it is noticed that the anomalous drop in R_H below T_{mag} is diminished in the 2.5% and 7.5% samples, and is absent in the 20% sample: as the Sn concentration is increased the RuO_2 layer becomes well localized below T_{mag}, reflecting significantly reduced conductivity at all temperatures. The changes in $R_H(290)$ and S_{290} may then be explained quite simply: the introduction of Sn dopes a few extra holes into the CuO_2 layer, increasing p_{Cu} and raising T_c by ~ 4 K, but also drives the RuO_2 layer more insulating. Thus while R_H^{Cu} probably decreases slightly, the overall Hall-effect increases as the RuO_2 layer no longer provides a parallel conduction pathway. The slight increase in p_{Cu}, which would normally decrease the measured TEP, is balanced by the decreasing σ_{Ru}, which removes the reduction of the TEP by the RuO_2 layer, leaving it relatively unchanged overall. Certainly, the increase in doping is far smaller than one would expect from substituting Sn^{4+} for Ru^{5+}, suggesting that the mean valency of the Ru ion is less than $5+$. This conclusion is supported by recent x-ray-absorption near-edge spectroscopy (XANES) measurements.[33]

The reduction in the room-temperature R_H of pure $RuSr_2GdCu_2O_8$, due to conductivity in the RuO_2 layer, was estimated to be of the order of 30%. This is entirely consistent with the rise in R_H observed as the Sn concentration is increased to 20%, assuming that $\sigma_{\mathrm{Ru}} \rightarrow 0$. The 40% Sn-doped sample does not fit well into this picture, having a much larger R_H at all temperatures. Given the much larger resistivity of this sample and its drastically reduced T_c, it is possible that some $Sn \leftrightarrow Cu$ substitution has occurred, reducing the CuO_2 layer doping state, or that there are significant impurities present.

2. Nb-doped $RuSr_2GdCu_2O_8$

Nb also substitutes for Ru in the $RuSr_2GdCu_2O_8$ structure, but has a dramatically different effect on the transport properties. In contrast to the Sn ion, which has a charge of $4+$, Nb is believed to substitute in its usual $5+$ state,[38] and thus for an average Ru valency of less than 5 will remove holes from the system, further underdoping it. The room-temperature TEP bears this out, showing a large increase proportionate with Nb doping (see Fig. 3) and confirming that the CuO_2 layer is progressively underdoped by the substitution of Nb. This conclusion is supported by the commensurate increase in the Hall effect and the rapid reduction of T_c, which is 19 K for the 10% sample and below 1.5 K (if present at all) in the 20% sample.

The effect of Nb doping on the Ru layer is less clear. The Hall effect of the 10% sample displays a maximum near T_{mag}, suggesting increased RuO_2 conductivity below this temperature, but the drop is not as clear as in the undoped

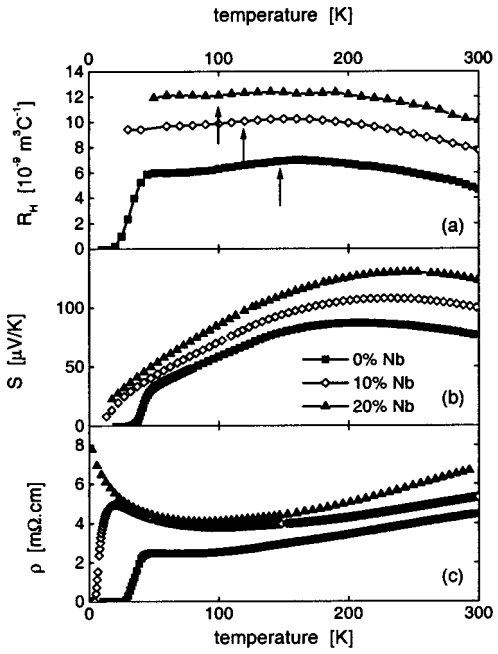

FIG. 3. (a) Hall-effect, $R_H(T)$, (b) thermopower, $S(T)$, and (c) resistivity, $\rho(T)$, data for Nb-doped $RuSr_2GdCu_2O_8$.

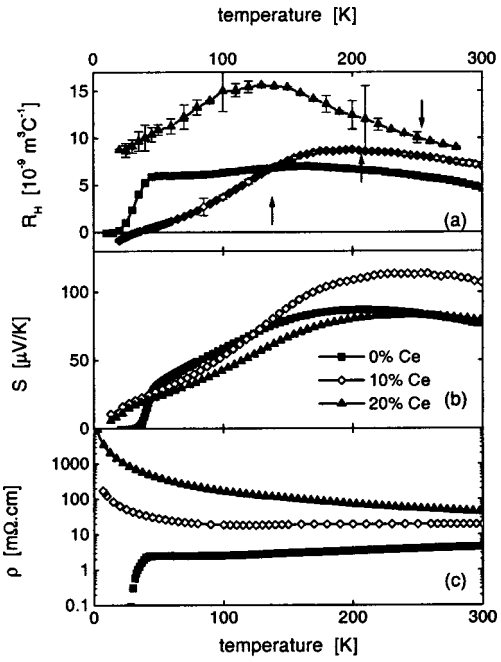

FIG. 4. (a) Hall-effect, $R_H(T)$, thermopower, $S(T)$, and resistivity, $\rho(T)$, data for Ce-doped $RuSr_2GdCu_2O_8$. The large error bars shown on the 20% Ce Hall data points result from the exceptionally large resistivity of the sample making balancing difficult at low temperatures. The error bars shown on the 10% Ce data points are more typical.

sample. For 20% Nb↔Ru substitution R_H rises to a more or less constant value of 1.2×10^{-8} m^3 C^{-1} below 200 K, and there is no sign of a significant change at T_{mag}. The conclusion from the TEP and Hall-effect data, then, is that the transition from localized to itinerant behavior of the RuO_2 layer is suppressed by the addition of Nb, as it is by the addition of Sn.

The resistivity, on the other hand, shows surprisingly little difference between the 10% and 20% samples—in fact the residual resistivity (extrapolated from the linear high-temperature data) actually *decreases*. A possible scenario consistent with this result is that the RuO_2 layer becomes *more* itinerant both above and below T_{mag} as the Nb level is increased. However, if this were the case, the increased σ_{Ru} would be expected to suppress both R_H and S below the CuO_2 plane values. In fact, for $T_c=19$ K and $T_c^{max}\approx100$ K, the universal relationship between S_{290} and T_c predicts $S_{290}^{\mathrm{Cu}}\sim100$ $\mu\mathrm{V\,K^{-1}}$, as observed. Thus, while the increased S and R_H and the reduced T_c are consistent with a reduced hole concentration in the CuO_2 layer and a localized RuO_2 layer, the relatively good conductivity of the 20% Nb-doped sample is not. One possible explanation is that the behavior of the resistivity is extrinsic to the bulk in the 20% Nb sample, resulting from either increased grain-boundary conductivity, or increased sample density.

3. Ce-doped $RuSr_2GdCu_2O_8$

Unlike Nb and Sn, which substitute for Ru, Ce substitutes for Gd in the layer separating the two CuO_2 planes, and so would be expected to affect these more than the RuO_2 layers from which it is relatively remote. The Ce ion is expected to be in the $4+$ state in $RuSr_2GdCu_2O_8$, as it is in the structurally similar compound $RuSr_2(Gd_{1+x}Ce_{1-x})Cu_2O_{10}$;[39] hence its substitution for Gd^{3+} should further underdope the material.

Two samples (10% and 20% Ce↔Gd) were measured, and, of all the doped samples studied, these exhibit the most remarkable and revealing transport properties: a large drop in R_H below T_{mag} (in fact becoming negative in the 10% sample below ~30 K), and a large TEP at room temperature which, like the Hall-effect, drops very rapidly below T_{mag}. These data are shown in Fig. 4, along with the resistivities of the two samples.

We note first that, as with other electron doping substitutions (Ce for Gd, La for Sr, and hydrogen doping), T_{mag} is driven upwards. This appears to reflect an increasing Ru^{4+} fraction. The 10% Ce sample will be dealt with first. As with the undoped sample, the departure from cupratelike properties below T_{mag} indicates a transition from localized to itinerant behavior in the RuO_2 layer. In this case, however, the room-temperature TEP $S_{290}=110$ $\mu\mathrm{V\,K^{-1}}$ indicates a much lower CuO_2 layer carrier concentration of $p\sim0.03$ holes/Cu. This is consistent with the increased Hall coefficient, which is probably still depressed from the true CuO_2 value by residual conductivity in the RuO_2 layer, and the large resistivity with its insulating upturn at low temperature. Having concluded that p, and hence σ_{Cu}, is much lower than in the undoped sample, the reason for the dramatic effects seen in R_H and S below T_{mag} becomes clear: the ratio $\sigma_{\mathrm{Ru}}/\sigma_{\mathrm{Cu}}$ is much larger in the Ce-doped sample at low temperature, allowing the intrinsic RuO_2 layer properties to dominate the behavior.

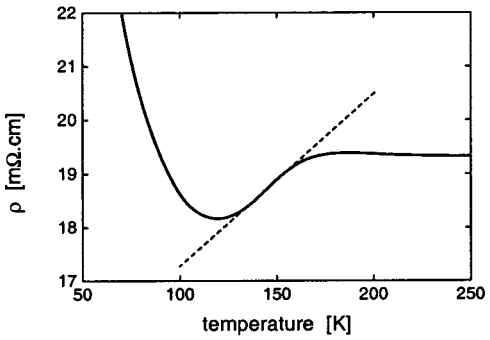

FIG. 5. Enlarged view of the resistivity of the 10% Ce-doped $RuSr_2GdCu_2O_8$ sample showing T-linear resistivity below T_{mag}.

The effect of changes in σ_{Ru}/σ_{Cu} is greater for R_H than S, but for these samples the increased σ_{Ru} depresses the S_{Cu} contribution to the total TEP so much that S_{Ru} dominates below 50 K. The basis for this assertion is the double maximum in dS/dT: initially, at low temperatures, $S(T)$ follows a curve reasonably consistent with the TEP of $SrRuO_3$. This contribution is trending towards saturation at a value of $\sim 40\ \mu V\,K^{-1}$; however, above 50 K increasing σ_{Cu} allows S_{Cu} to contribute, and the overall TEP then rises more rapidly.

The same qualitative treatment may be applied successfully to the Hall-effect data, though in order to explain the negative values below ~ 30 K it is necessary to assume a negative Hall coefficient for the RuO_2 layer of around $-1 \times 10^{-9}\ m^3\ C^{-1}$. Examining typical data from the $Sr_{n+1}Ru_nO_{3n+1}$ series one finds that R_H of $Sr_3Ru_2O_7$ remains positive at all temperatures, while that of Sr_2RuO_4 becomes negative below 20 K, but reaches just $-1 \times 10^{-10} m^3\,C^{-1}$ near 1 K. However, $SrRuO_3$, which has the most similar ferromagnetic RuO_2 layer to $RuSr_2GdCu_2O_8$, has a negative R_H below 100 K, reaching a field-dependent value of $\sim -1 \times 10^{-9} m^3\,C^{-1}$ below 60 K.[20] Thus the value of R_H observed in the Ce-doped sample at low temperature is the same order of magnitude as that in $SrRuO_3$, confirming that the RuO_2 layer dominates the transport properties. It is interesting to note that, though it may not be a large effect, Ce substitution for Gd should drive the mean Ru valence closer to $4+$, as it is in $SrRuO_3$.

Turning now to the resistivity, one encounters a problem: if the RuO_2 layer is indeed metallic below T_{mag}, why does the resistivity increase so dramatically as $T \to 0$? There are two possible answers to this question: either both the RuO_2 and CuO_2 layers are at least semiconducting, but such that $\sigma_{Ru}/\sigma_{Cu} > 1$, or it may be that insulating grain boundaries cause the upturn. The second of these scenarios seems more likely. In this case the TEP and Hall effect, being much less sensitive to intergrain connectivity, are determined by a weakly metallic intrinsic σ_{Ru}. Support for this conclusion is provided by close examination of the resistivity (Fig. 5) which shows an extended metallic region below T_{mag}.

This type of behavior is not uncommon in $RuSr_2GdCu_2O_8$—in fact extrinsic upturns in resistivity are observed in poorly annealed undoped samples. Interestingly though, transport measurements on $SrRuO_3$ also show a minimum in resistivity below T_{Curie} in samples where there is some disorder in the RuO_2 layer.[40] The temperature at which the minimum occurs, and the magnitude of the upturn below it both increase with RuO_2 layer disorder: in good quality films the highest-temperature minimum observed is 40 K, coincident with the maximum residual resistivity.[40]

The 20% Ce-doped sample deviates nontrivially from the scenario for the 10% Ce sample: R_H is higher at room temperature, as one would expect for even greater underdoping caused by the increase in Ce content, but S_{290} is actually *lower* than that of the 10% sample, apparently implying an increased hole concentration. In the absence of a clear resolution we prefer not to speculate on these changes which could just arise from disorder near a solubility limit.

4. Calculation of $\beta(T)$ in Ce-doped $RuSr_2GdCu_2O_8$

The ratio $\beta(T) = \sigma_{Ru}(T)/\sigma_{Cu}(T)$ may be extracted from the data for the 10% Ce-doped sample using the two-band model, as described for the undoped material. As in the previous calculation, typical $S^{Cu}(T)$ and $R_H^{Cu}(T)$ data are matched to the high-temperature $RuSr_2GdCu_2O_8$ data, where σ_{Ru} is assumed to be small compared with σ_{Cu} and the overall properties reflect those of the CuO_2 layer most strongly. The deviation from cupratelike behavior at lower temperatures is then used to extract the ratio $\beta(T)$.

For this sample, $S^{Cu}(T)$ data were taken as 1.05 times $S(T)$ measured on a sample of underdoped sintered $YBa_2Cu_3O_{7-\delta}$, with $\delta \simeq 0.6$.[26] $R_H^{Cu}(T)$ data were taken as 1.16 times R_H measured on a similar sample with $\delta \simeq 0.62$.[41] R_H and S are particularly strong functions of doping in this region of the phase diagram: the good agreement in the values of δ required for the two sets of data to match those of $RuSr_2GdCu_2O_8$ suggests that the assumption of negligible σ_{Ru} at high temperature is reasonable.

The TEP of the RuO_2 layer is approximated by that of sintered $SrRuO_3$, as before. As the Hall effect becomes negative at low temperatures in Ce-doped $RuSr_2GdCu_2O_8$ taking $R_H^{Ru} \simeq 0$, as was done for the undoped material, will not work. Instead a rough approximation to data for $SrRuO_3$ is used,[20] which shows a field-dependent value of $\sim -1 \times 10^{-9}$ at 20 K.

The measured and estimated data together with the results of the calculations are shown in Fig. 6. Above 50 K there is remarkable agreement between $\beta(T)$ calculated from the TEP data (β_{TEP}) and that calculated independently from the Hall-effect data (β_{Hall}), lending confidence both to the model and to the estimated $R_H(T)$ and $S(T)$ data for the RuO_2 and CuO_2 layers. Below 50 K the agreement is not so good: β_{Hall} carries on increasing, a direct result of R_H^{1212} becoming very close to the estimated R_H^{Ru} at low temperatures. S^{1212} does not approach the estimated S^{Ru} as closely, and hence β_{TEP} does not continue to increase. Emerging clearly from these data is a large increase in β below T_{mag}. At 50 K $\sigma_{Ru}/\sigma_{Cu} \sim 1.9$, whereas for the undoped material the increase in σ_{Ru}/σ_{Cu} is just 0.3. The properties of the RuO_2 layer dominate the overall transport properties of $RuSr_2GdCu_2O_8$ below ~ 90 K in this 10% Ce-doped sample.

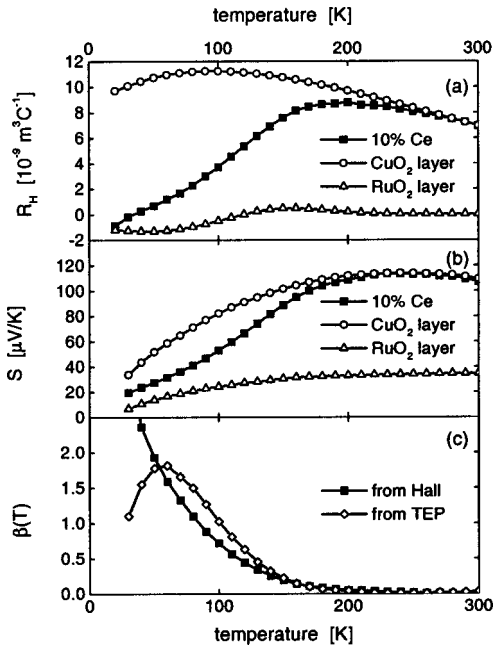

FIG. 6. (a) Hall-effect and (b) thermopower data for $RuSr_2Gd_{0.9}Ce_{0.1}Cu_2O_8$, together with the estimated RuO_2 and CuO_2 layer values, as described in the text. Panel (c) shows the ratio $\beta = \sigma_{Ru}/\sigma_{Cu}$ calculated in the two-band model from thermopower and, independently, from the Hall effect.

5. Other doped samples

The remainder of the doped samples studied contained Y, Dy, and Eu on the Gd site, plus a 5% Li-doped sample, in which Cu is substituted. The transport data for all these samples are shown in Fig. 7.

The Hall effect shows the ''usual'' anomalous downturn below T_{mag} in all these samples. The magnitude of the downturn, due to the transition to a more itinerant Ru layer, is approximately constant, leading to the conclusion that doping the Cu and Gd sites does not greatly affect the localization of carriers in the RuO_2 layer.

Substituting a small amount of Li^+ for Cu^{2+} causes virtually no change in the TEP, but depresses T_c by ≈ 20 K. The Hall effect of this sample is slightly larger than that of the undoped sample, possibly due to some cross substitution of Li with Ru, depressing σ_{Ru}, or a slight decrease in the CuO_2 layer carrier concentration. These results are consistent with Li^+ acting as a pair breaker in the CuO_2 layer, but with little other effect on transport properties. The rate of suppression of T_c with Li substitution in $RuSr_2GdCu_2O_8$, ~ 4 K/%, is about one quarter of that observed in underdoped $YBa_2Cu_3O_{7-\delta}$($\delta = 0.4$) when either Li or Zn is substituted for Cu.[42] However the concentration of Li in the $RuSr_2GdCu_2O_8$ sample studied is nominal, and the difference in the rate of suppression may simply reflect loss of Li by vaporization during the long synthesis and anneal.

The isovalent substitution of Y or Dy for Gd actually causes a slight *decrease* in the TEP of $RuSr_2GdCu_2O_8$, these being the only substitutions studied to do so. The implied increase in the doping level of the CuO_2 layers, presumed to arise from an ion-size effect, is confirmed by the increased

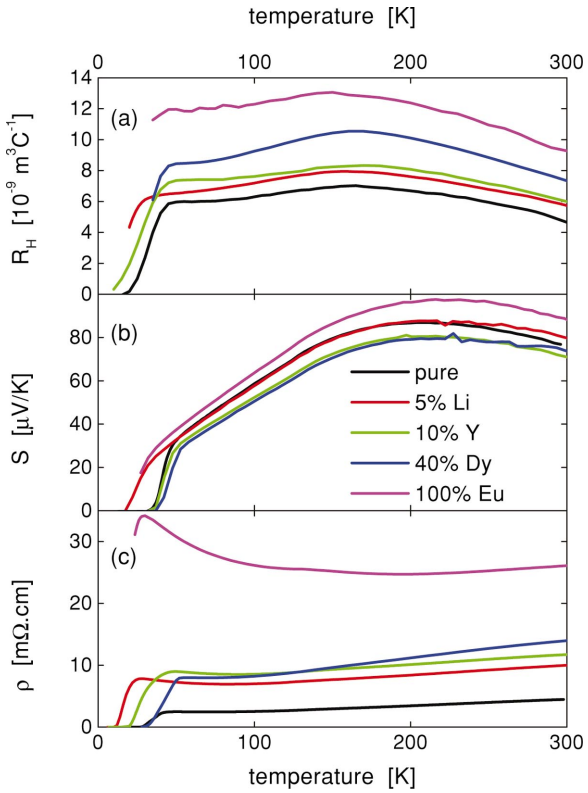

FIG. 7. (Color) (a) Hall-effect, $R_H(T)$, (b) thermopower, $S(T)$, and (c) resistivity, $\rho(T)$, data for $RuSr_2GdCu_2O_8$ with 10% Y, 40% Dy, and 100% Eu substituted for Gd, or 5% Li substituted for Cu.

T_c in these samples—≈ 2 K (10% Y) and 6 K (40% Dy) higher than in the undoped sample as seen by both resistivity and TEP measurements. However, the magnitude of the Hall-effect is larger for these samples than for the undoped ones. Having argued that the CuO_2 layer is less underdoped in these two samples, this effect may only arise from a decrease in the conductivity of the RuO_2 layer, partially removing the ''shorting'' of the CuO_2 layer Hall-effect.

Full substitution of Eu for Gd causes an increase in S_{290} to 90 μV K^{-1}, T_c as measured by the TEP or resistivity drops significantly, and R_H is greatly increased. All these results suggest a drop in the CuO_2 layer hole concentration, again consistent with the above-noted ion-size effect, perhaps coupled with a decrease in σ_{Ru}. Consistent with this interpretation, the resistivity of this sample is much less metallic than that of the others (which are all metallic, with magnitudes two to three times the well-annealed undoped sample).

IV. DISCUSSION

The Hall-effect and TEP data described in this paper provide strong evidence for a transition from very poorly metallic to more itinerant behavior in the RuO_2 layer below T_{mag}. Results from substituted $RuSr_2GdCu_2O_8$ samples confirm this picture. The universal relationship between S_{290} and p_{Cu} appears to hold in $RuSr_2GdCu_2O_8$ as a result of the low σ_{Ru} at room temperature, though below T_{mag} both S and R_H are reduced by the shorting of the S_{Cu} by RuO_2 layer.

The two-band model proposed is successful in explaining most of the existing data qualitatively: the anomalies, which lie mainly in resistivity data, are most likely due to grain-boundary and density effects. The quantitative agreement is also reasonably good. The results support a picture in which the RuO_2 layer in the pure compound is localized above T_{mag}, with $\sigma_{Ru} \sim 0.1\sigma_{Cu}$, but becomes more conducting below T_{mag}, mirroring the behavior of other ruthenates.

The transition from localized to itinerant RuO_2 layer behavior at T_{mag} in the undoped compound may be modified by substituting Ru with Sn or Nb. Sn increases the doping level of the CuO_2 layers, raising T_c and suppressing T_{mag}, and simultaneously drives the RuO_2 layer more insulating. Nb underdopes the CuO_2 layers, lowering T_c, and also appears to drive the RuO_2 layer insulating, though the 20% sample does not show the expected semiconducting resistivity. These results imply an initial Ru valence lying between $4+$ and $5+$, in agreement with XANES data which may be modeled as an admixture of 40% Ru^{4+} and 60% Ru^{5+}.[33]

As might be expected, doping of the Cu site has little effect on T_{mag} or the transport properties of the RuO_2 layer. Li^+ acts as a pair-breaking impurity in the CuO_2 layer and causes a depression of T_c in line with its behavior in other cuprates. Isovalent doping of the Gd site with other lanthanide elements changes the CuO_2 layer doping level, with a remarkably strong variation in T_c. This appears to be a ion-size doping effect. Altervalent substitution of Ce for Gd rapidly reduces the doping level of the CuO_2 layers and drives the material nonsuperconducting. In all but the Ce-doped samples, the conductivity of the RuO_2 layer only ever reaches a modest fraction of that of the CuO_2 layer. In the 10% Ce-doped sample the more heavily underdoped CuO_2 layer has an insulating upturn at low temperature, while the RuO_2 layer remains more metallic, and so the ratio of their conductivities reaches at least 1.9.

V. CONCLUSIONS

To a first approximation the electronic properties of the CuO_2 layer in $RuSr_2GdCu_2O_8$ are the same as those of similar CuO_2 layers in other high-T_c cuprate superconductors in all respects. This conclusion is supported by the resistivity, TEP, and Hall-effect data presented here, and by results on the specific-heat jump at T_c. On a more detailed level, magnetotransport measurements reveal an interaction between the carriers in these layers and the magnetization of the RuO_2 layer. This interaction, with an energy which would seem to be of the same order as the SC energy gap,[10] is not sufficient to destroy superconductivity.

The electronic properties of the RuO_2 layer appear to bear a remarkable similarity to those observed in the ruthenate $SrRuO_3$. At room temperature the conductivity of the layer is perhaps 10% of that of the CuO_2 layer, with $k_F l_{Ru} \approx 0.2$, indicating very badly metallic or localized behavior. Below T_{mag} the conductivity of the layer rises significantly—by at least $0.3\sigma_{Cu}$. This increase raises the weighting of the RuO_2 layer properties relative to those of the CuO_2 layer in the admixture that determines the overall transport properties of $RuSr_2GdCu_2O_8$. As the Hall-effect and TEP of the RuO_2 layer are both considerably smaller than those in the CuO_2 layer the result is a drop in both R_H and S below T_{mag}. In pure $RuSr_2GdCu_2O_8$, and also in most of the substituted variants studied, σ_{Ru} remains lower than σ_{Cu} over the whole temperature range. For the Ce-doped samples studied, however, the CuO_2 layer becomes insulating at low temperatures, allowing the poorly metallic RuO_2 layer to dominate the conductivity, and its intrinsic transport properties to show strongly in the overall R_H and S of the material.

The two-band model of parallel conduction in the RuO_2 and CuO_2 layers has been very successful in modeling the transport properties observed in all the $RuSr_2GdCu_2O_8$ samples studied, and it has been possible to describe well the effects of doping the different atomic sites. The inferred mixed valency of Ru, together with the onset of itinerancy at the magnetic transition, suggests a possible role of a double-exchange mechanism in the magnetic interactions but also raises the possibility of charge ordering in these compounds at appropriate doping levels.

ACKNOWLEDGMENTS

This work was supported by the U.K. Engineering and Physical Sciences Research Council and the New Zealand Marsden Fund for research (JLT) and travel funds (CB).

[1] L. Bauernfeind, W. Widder, and H.F. Braun, J. Low Temp. Phys. **105**, 1605 (1996).
[2] J.L. Tallon, C. Bernhard, and J.W. Loram, J. Low Temp. Phys. **117**, 823 (1999).
[3] C. Bernhard, J.L. Tallon, Ch. Niedermayer, Th. Blasius, A. Golnik, E. Bruecher, R.K. Kremer, D.R. Noakes, C.E. Stronach, and E.J. Ansaldo, Phys. Rev. B **59**, 14 099 (1999).
[4] A. Fainstein, E. Winkler, and A. Butera, Phys. Rev. B **60**, R12 597 (1999).
[5] C. Bernhard, J.L. Tallon, E. Bruecher, and R.K. Kremer, Phys. Rev. B **61**, 14 960 (2000).
[6] J.E. McCrone, J.R. Cooper, J.W. Loram, and J.L. Tallon (unpublished).
[7] O. Chmaissem, J.D. Jorgensen, H. Shaked, P. Dollar, and J.L. Tallon, Phys. Rev. B **61**, 6401 (2000).
[8] J. Lynn, B. Keimer, C. Ulrich, C. Bernhard, and J.L. Tallon, Phys. Rev. B **61**, R14 964 (2000).
[9] H. Takigawa, J. Akimitsu, H. Kawano-Furukawa, and H. Yoshizawa, J. Phys. Soc. Jpn. **70**, 333 (2001).
[10] J.E. McCrone, J.R. Cooper, and J.L. Tallon, J. Low Temp. Phys. **117**, 1199 (1999).
[11] M. Pozek, A. Dulcic, D. Paar, A. Hamzic, M. Basletic, E. Tafra, G.V.M. Williams, and S. Kramer, Phys. Rev. B **65**, 174514 (2002).
[12] Y. Tokunaga, H. Kotegawa, K. Ishida, Y. Kitaoka, H. Takagiwa, and J. Akimitsu, Phys. Rev. Lett. **86**, 5767 (2001).

[13] J. Tallon, C. Bernhard, M.E. Bowden, P.W. Gilberd, T. Stoto, and D.J. Pringle, IEEE Trans. Appl. Supercond. **9**, 1696 (1999).
[14] J.R. Cooper, C. Rizzuto, and G. Olcese, J. Phys. (Paris) **32**, 1136 (1971).
[15] R. Resel, E. Gratz, A.T. Burkov, T. Nakama, M. Higa, and K. Yagasaki, Rev. Sci. Instrum. **67**, 1970 (1996).
[16] S.D. Obertelli, J.R. Cooper, and J.L. Tallon, Phys. Rev. B **46**, 14 928 (1992).
[17] J.E. McCrone, Ph.D. thesis, University of Cambridge, 2001.
[18] C.M. Hurd, *The Hall Effect in Metals and Alloys* (Plenum, New York, 1972).
[19] R.D. Barnard, *Thermoelectricity in Metals and Alloys* (Taylor and Francis, London, 1972).
[20] H.C. Yang, S.H. Liu, L.M. Wang, and H.E. Horng, J. Appl. Phys. **85**, 5792 (1999).
[21] A.P. Mackenzie, N.E. Hussey, A.J. Diver, S.R. Julian, Y. Maeno, S. Nishizaki, and T. Fujita, Phys. Rev. B **54**, 7425 (1996).
[22] R.S. Perry, L.M. Galvin, A.P. Mackenzie, D.M. Forsythe, S.R. Julian, S.I. Ikeda, and Y. Maeno, Physica B **284**, 1469 (2000).
[23] B. Wuyts, V.V. Moshchalkov, and Y. Bruynseraede, Phys. Rev. B **53**, 9418 (1996).
[24] A. Carrington, D.J.C. Walker, A.P. Mackenzie, and J.R. Cooper, Phys. Rev. B **48**, 13 051 (1993).
[25] I.R. Fisher, P.S.I.P.N. de Silva, J.W. Loram, J.L. Tallon, A. Carrington, and J.R. Cooper, Physica C **235-240**, 1497 (1994).
[26] J.R. Cooper and J.W. Loram, J. Phys. I **6**, 2237 (1996).
[27] Y. Sun, G. Strasser, E. Gornik, and X.Z. Wang, Physica C **223**, 14 (1994).
[28] R. Jin and H.R. Ott, Phys. Rev. B **57**, 13 872 (1998).
[29] A. Carrington, A.P. Mackenzie, C.T. Lin, and J.R. Cooper, Phys. Rev. Lett. **69**, 2855 (1992).
[30] H. Yoshino, K. Murata, N. Shirakawa, Y. Nishihara, Y. Maeno, and T. Fujita, J. Phys. Soc. Jpn. **65**, 1548 (1996).
[31] G.V.M. Williams and S. Kramer, Phys. Rev. B **62**, 4132 (2000).
[32] A. Butera, A. Fainstein, E. Winkler, and J.L. Tallon, Phys. Rev. B **63**, 054442 (2001).
[33] R.S. Liu, L.-Y. Jang, H.-H. Hung, and J.L. Tallon, Phys. Rev. B **63**, 212507 (2001).
[34] J.R. Cooper, S.D. Obertelli, P.A. Freeman, D.N. Zheng, J.W. Loram, and W.Y. Liang, Supercond. Sci. Technol. **4**, S277 (1991).
[35] I.R. Fisher and J.R. Cooper, Physica C **272**, 125 (1996).
[36] A. Carrington and J.R. Cooper, Physica C **219**, 119 (1994).
[37] A.C. Maclaughlin and J.P. Attfield, Phys. Rev. B **60**, 14 605 (1999).
[38] A.C. Maclaughlin, V. Janowitz, J.A. McAllister, and J.P. Attfield, Chem. Commun. (Cambridge) **14**, 1331 (2000).
[39] I. Felner, U. Asaf, C. Godart, and E. Alleno, Physica B **261**, 703 (1999).
[40] L. Klein, J.S. Dodge, C.H. Ahn, G.J. Snyder, T.H. Geballe, M.R. Beasley, and A. Kapitulnik, Phys. Rev. Lett. **77**, 2774 (1996).
[41] A. Carrington, Ph.D. thesis, University of Cambridge, 1993.
[42] J. Bobroff, W.A. MacFarlane, H. Alloul, P. Mendels, N. Blanchard, G. Collin, and J.-F. Marucco, Phys. Rev. Lett. **83**, 4381 (1999).